Research Article

Manikandan Dhayalan*, Malathi Selvaraj, Karthick Kumar B, Mohammed Riyaz S.U., and Mika Sillanpää*

Eco friendly synthesis and characterization of zinc oxide nanoparticles from *Aegle marmelos* and its cytotoxicity effects on MCF-7 cell lines

https://doi.org/10.1515/nanofab-2020-0104
Received May 07, 2021; accepted Nov 19, 2021

Abstract: An attempt was made to synthesize zinc oxide gum white nanoparticles (ZnO-GWNPs) by the greenway approach using *Aegle marmelos* (Bael fruit) juice extract as a capping and reducing agent. Synthesis of ZnO-GWNPs by greener approach is safer, more economical, more energy-efficient, eco-friendlier, and less toxic than chemically synthesized counterparts. The optical properties of the ZnO-GWNPs were ascertained through UV-Vis spectroscopy, Fourier Transform-Infrared (FT-IR), X-ray diffraction (XRD), High-resolution transmittance electron microscopy (HR-TEM). A characteristic absorption peak at 385nm confirmed the presence of ZnO-GWNP using UV-Vis spectroscopy. FTIR spectrum revealed that the characteristic absorption peak of the Zn-O bond was observed at 467 cm-1. The XRD result for the ZnO showed the tendency of the three most intense diffraction peaks. The average crystallite size ZnO NPs at scattering angle (2θ) 22.89 and 32.15 was 39.14 and 26.08 nm and it showed the presence of miller indices of (100), (002), (101), (102) respectively. The EDX spectrum gave strong signals for zinc and oxygen indicating the occurrence of the nanoparticles in their oxide form rather than the pure zinc form. The SEM image showed the surface morphology of ZnO-GW NPs and the HR-TEM image showed the crystalline nature of ZnO-GW NPs. Cytotoxicity study of ZnO-GW NPs was determined against MCF-7 cell lines and the IC50 values were found to be 40 µg/mL and 60 µg/mL at 24 h and 48 h respectively.

Keywords: Greenway; Zinc oxide nanoparticles (ZnO-GW NPs); bael fruit extracts, Cytotoxicity

1 Introduction

Nanotechnology is an immensely developing field in science. It is conducted at the nano-meter scale to explore several disciplines in the field of research, such as physics, chemistry, material science and medicine [1, 2]. Nanoparticles are metal particles in nanoscale (1-99 nm) size and exhibit different structures like spherical, triangular, rod, *etc* [3, 4]. The main advantage of nanoparticles (NPs) is generally their larger surface to volume ratio when compared with micron-sized particles. Zinc oxide (ZnO) is a Federal Drug Administration (FDA) approved inorganic compound being used in wide range of commercial application such as food, cosmetics, textile and medicine. Zinc nanoparticles (ZnO NP) are widely used in nano optical and nano electrical fields because of their high catalytic activity, and also in food packaging and in medicine as antibacterial and anticancer agents [5, 6].

The production of nanoparticles through biosynthesis may actually produce a better defined size and morphology as compared to other physical and chemical methods of production [7]. *Aegle marmelos* is commonly known as bael belongs to the family Rutaceae. It is native in Indian subcontinent and south East Asia. The whole tree such as root, leaf, trunk, fruit, and seed are used extensively in Indian ayurveda and folk medicine as a traditional medicine to cure various human ailments [8] and diseases and scientific data also validated their therapeutic performance that includes free radical scavenging, antioxidant, inhibition of

***Corresponding Author: Manikandan Dhayalan:** Anticancer Bioscience, Ltd. Tianfu International Biotown Chengdu, 610000, China; Email: manikandandhayalan88@gmail.com
***Corresponding Author: Mika Sillanpää:** Environmental Engineering and Management Research Group, Ton Duc Thang University, Ho Chi Minh City, Vietnam; Faculty of Environment and Labour Safety, Ton Duc Thang University, Ho Chi Minh City, Vietnam; Email: mika.sillanpaa@tdtu.edu.vn
Malathi Selvaraj: Centre for Advanced Studies in Botany, Guindy Campus, University of Madras, Chennai-600 025 India
Karthick Kumar B: Department of Textile Technology, A.C.Tech, Anna University, Chennai-600025, Tamilnadu, India
Mohammed Riyaz S.U.: Animal Tissue culture unit, PG & Research Department of Biotechnology, Islamiah College (Autonomous), Newtown, Vaniyambadi-635752, Tamilnadu, India

lipid per oxidation, antibacterial, antiviral, anti-diarrheal, gastro protective, anti-ulcerative colitis, hepatoprotective, anti-diabetic, and cardio protective uses [9]. Bael is reported to contain biologically important phytochemical-saegeline, marmelosin, luvangetin, auraptene, psoralen, marmelide, and tannin [10].

N D Krupa *et al.*, reported the synthesis of spherical shaped silver NPs with bael fruit extract for antibacterial activity on thin films used in food packaging industry [11]. In 2015, K J Rao *et al.*, demonstrated the green synthesis of gold and silver NPs using bael extract [12]. Recently Devi *et al.*, reported the synthesis of AgNPs from bael fruit as a potential antibacterial agent against human pathogens [13]. Thus, the studies showed that nanoparticles biosynthesised from bael extract possess a good pharmaceutical activity and can be further researched in neglected diseases. The synthesis of zinc metal nanoparticles (Zn NPs) by bael fruit is considered to be clean, cost effective, non-toxic and environmentally acceptable when compared with physically or chemically synthesized ZnO nanoparticles and believed to expect pharmacological activities. In this paper, we have studied the prospect of green synthesis of ZnO-GWNPs using bael fruit extracts. The morphology, crystal size, functional groups were investigated and the anticancer activity of the biosynthesized ZnO-GW NPs was tested against MCF7 cancer cell line.

2 Methods

2.1 Chemical and reagents

All chemicals utilized in this study were of analytical grade. Zinc acetate $Zn(CH_3CO_2)_2$and (3-[4,5-dimethylthiazol-2-yl]-2, 5-diphenyl tetrazolium bromide) were purchased from Merck, Mumbai, India. Cell lines of MCF-7 were obtained from National Centre for Cell Science (NCCS), Pune, India. Foetal Bovine Serum (FBS) was obtained from Sigma-Aldrich Chemicals, USA. Phenol red, Foetal Calf serum, L-glutamine, Trypsin, Glucose, Rosewell Park Memorial Institute Medium (RPMI), Nutrient Agar (NA), Barium Chloride, Casein acid Hydrolysate, Starch soluble, Agar were obtained from Himedia Laboratories, Pune, India.

2.2 Green synthesis of ZnO-GW nanoparticles

Matured bael fruit were collected from the region of Pollachi in Coimbatore district, Tamil Nadu, India during the month of December 2019. The bael fruit slices were thoroughly washed and dried in the oven at 60°C for one week. Then they were ground with a manual mixer to obtain fine powders. Twenty gram of the powder was heated in a closed flask containing 500 mL distilled water for a period of 1h at 90°C under moderate agitation. After which the coloured solution was cooled to room temperature and filtrated with a WhatmanNo.1 filter paper. This filtrate would serve as bael gum extract and freshly prepared bael gum extract (325 mL) was mixed with a 100 mL of zinc acetate (1M) solution under continuous stirring at 60°C for 1 h. The colour of the solution turned to red. The resultant precipitate was stand in mother liquor overnight. The precipitate has been separated using a centrifuge and washed many times with demineralised water. The synthesized particles were dried in oven at 60°C during 48 h and were used for further experiments. The obtained ZnO Nano powder synthesized with green ways method is hereafter termed as ZnO-GW NPs.

2.3 Characterization of ZnO-GW nanoparticles

The synthesis of ZnO-GW NPs were monitored by periodic sampling of the reaction mixture in double beam UV/Vis spectrophotometer (UV-1601, Shimadzu Corporation, Japan), at a wavelength range 200 to 900 nm at 1 nm resolution. The bio molecules responsible for the synthesis of ZnO-GW NPs nanoparticles and capping structure on the nanoparticles were determined through FTIR analysis by KBr (FTIR grade) pellet method (Perkin Elmer, USA, Model Y 40). The FTIR analysis was performed with KBr pellets in the range of 400 cm^{-1}–4000 cm^{-1} with 32 scans at a resolution of 2 cm^1. The crystalline nature of the phyto synthesized nanoparticles was analyzed by subjecting the sample to X-ray diffractometer of an analytical X'pert PRO diffractometer with monochromatic Cu-Kα1 radiation (λ = 1.5418 Å), 2θ ranging from 10° to 80°C in steps of 0.017°/s. The accelerating voltage was set at 40 kV and the current flux at 30 mA (Shimadzu, Japan). Complete separation of solid phase from aqueous solution was obtained by centrifugation using CRPM 2000, Rankim. The surface morphology of the material was studied. The size and shape of the nanoparticles were analysed using High resolution transmission electron microscopic analysis (FEI TECNAI G2S-TWIN, 250 Kv, FEI, USA). The sample preparation for HR-TEM analysis was carried out by filtering the synthesized nanoparticles through 0.2 µm sterile membrane filter (Uniflo TM, USA), and the filtrate was placed on the carbon coated copper grid. The excess solution was removed by

blotting with the cone of filter paper and observed under HR-TEM.

2.4 In Vitro Cytotoxicity (MTT) Assay

In vitro cytotoxicity of ZnO-GW NPs prepared using *Aegle marmelos* fruit extract was investigated by the conventional MTT reduction assay. MCF-7 cells (5×10^3) were seeded in flat-bottom 96-well plates for 24 h in 200 µL of RPMI with 10% FBS. After 24 h, various concentrations of ZnO-GW NPs (20-100 µg/mL) were added to the wells and subsequently incubated at 37°C for 24 h and 48 h. At the end of the incubation period, 10 µL MTT solution (5 mg/mL) was added to the wells, and the plate was incubated for 4 h. The supernatant was replaced by DMSO (150 µL) and incubated for 1h at room temperature, then the absorbance was measured at 545 nm using a scanning multi-well spectrophotometer UV-1601 spectrophotometer (Shimadzu, Japan). Trials were performed in triplicate and repeated three times. IC_{50} (half-maximal inhibitory concentration) value of ZnO GW nanoparticles, which inhibits 50% of the cells were found out using the following formula:

$$\text{Growth Inhibition} = \frac{\text{OD of control} - \text{OD of treated sample}}{\text{OD of control}} \quad (1)$$

3 Results and Discussion

3.1 Synthesis of ZnO-GW nanoparticles

The conversion of zinc acetate to ZnO by the aqueous bael fruit extract was marked by a visible colour change from deep green to red of the reaction mixture (Figure 1). The synthesis of ZnO-GW nanoparticles occurred rapidly after the addition of the extract to the zinc acetate solution. The formation of ZnO-GW nanoparticles in the reaction mixture, exhibiting a visible colour change, was confirmed by the occurrence of characteristic surface plasmon resonance (SPR) peak.

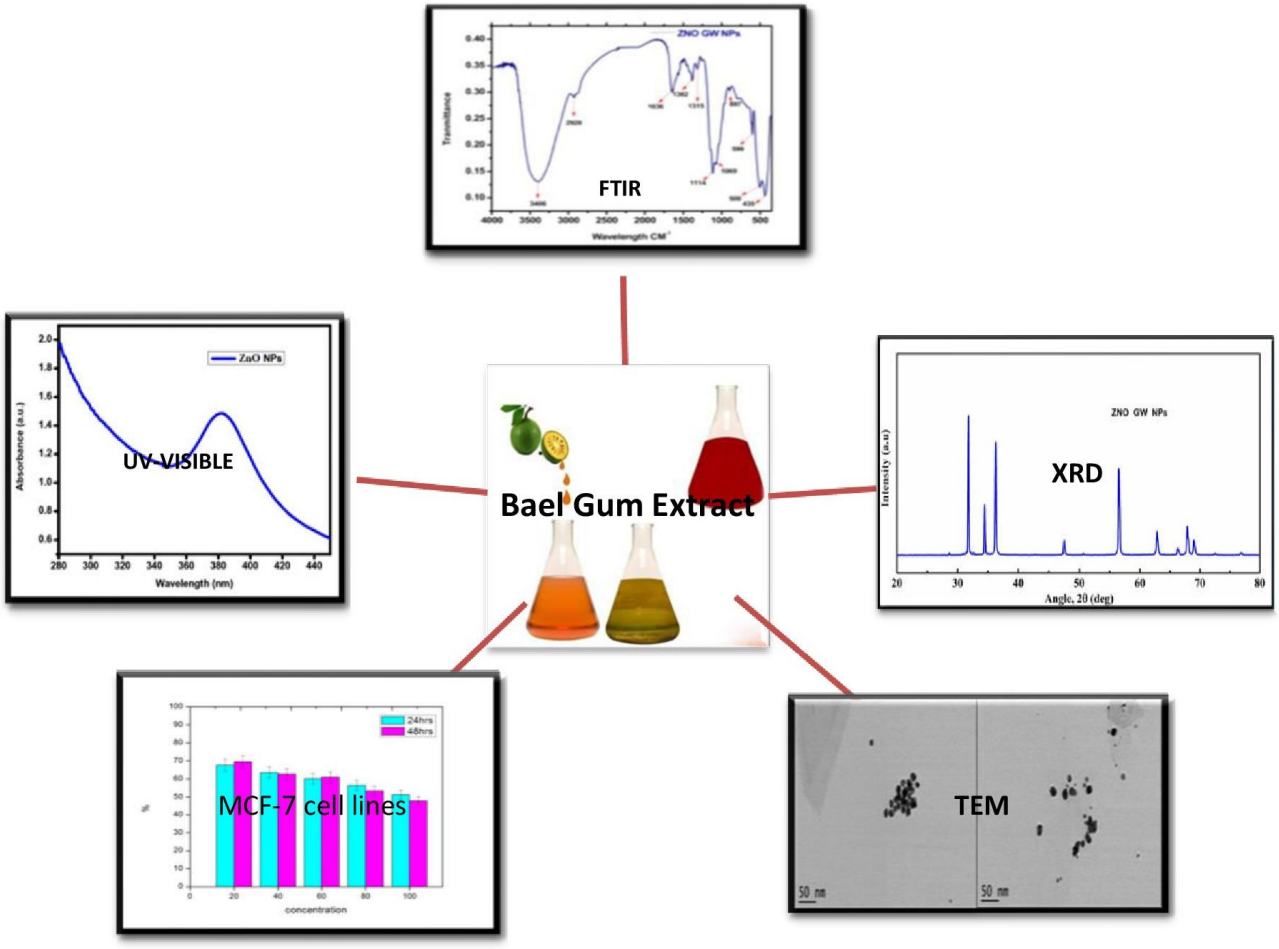

Figure 1: Graphical representation of synthesis of ZnO-GW nanoparticles.

3.2 UV-Vis Spectroscopy

Zinc oxide nanoparticles synthesized using *Aegle marmelos* fruit extract exhibited characteristic maximum absorbance at 385 nm (Figure 2). The wide bandwidth energy of 3.187 eV as estimated using E = hc/λ (h = planck constant; c = velocity of light; λ = absorption maxima) suggests the narrow size distribution of nanoparticles. Previously, ZnO NPs synthesized using *Aegle marmelos* extract and microwave irradiationmethod had an absorption maxima of 377 nm and 3.29 eV [14]. Similarly ZnO NPs synthesized using *Euphorbiajatropa* latex showed absorption maxima in the range of 300 to 400 nm and had a band width in the range of 3.1 to 4 eV [15].

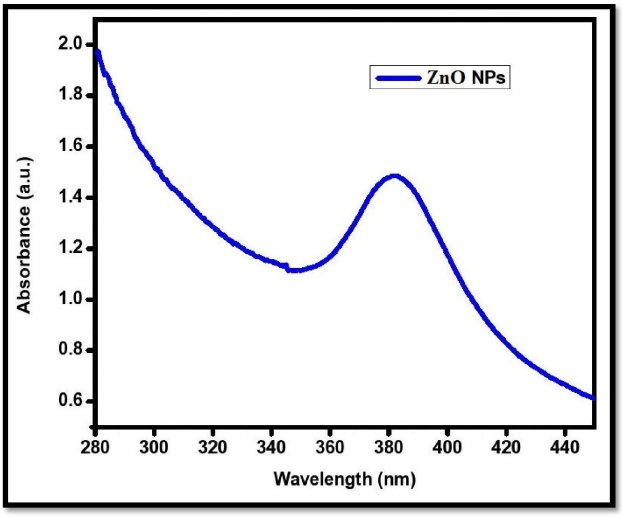

Figure 2: UV-Visible absorbance of *Bael fruit* extract showed characteristic peak of ZnO GW nanoparticles at 385nm.

3.3 Fourier transformed infrared spectroscopic (FTIR) analysis of ZnO- GW nanoparticles

FT-IR was carried out in order to find out the functional groups which are responsible for the reduction of zinc ions into nanoparticles and also ascertain the purity and nature of the nanoparticles. IR spectrum of ZnO-GW NPs shows that the strong and broad spectral bands observed at 3406 cm^{-1} was assigned to the N-H stretching which corresponds to aliphatic primary amine groups (Figure 3). The bands at 2928 cm^{-1} correspond to the C-H stretching vibrations which corresponds to alkane groups. The skeletal vibrations of the aromatic rings show band 1636 cm^{-1} which is assigned to C = C stretching vibrations which

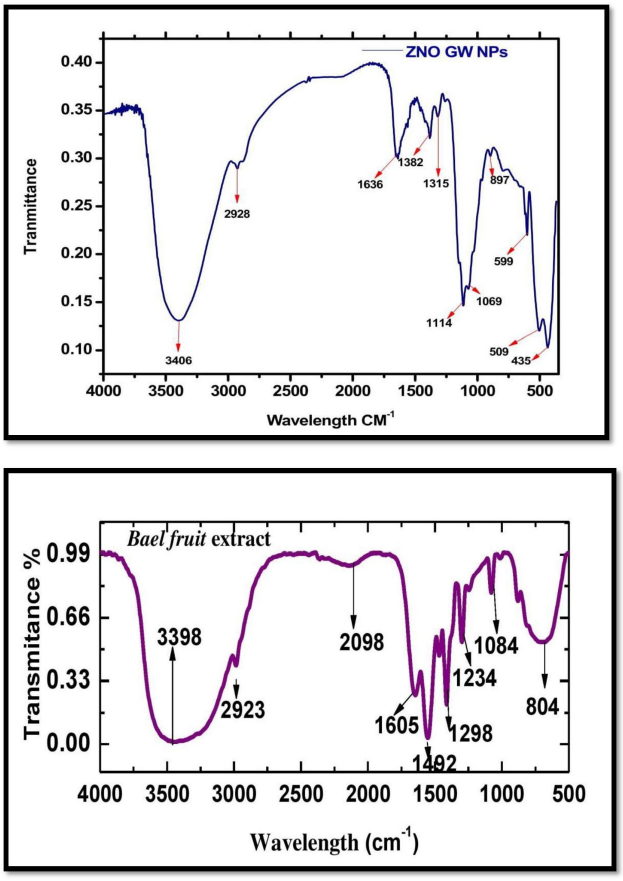

Figure 3: FTIR spectra of ZnO GW nanoparticles prepared using *Aeglemarmelos* (Bael fruit) fruit extract.

corresponds to alkenes [17]. The band at 1382 cm^{-1} corresponds to the asymmetric and symmetric (COO^-) carbonyl bonds [18, 19]. The band at 1315 cm^{-1} is due to C-O stretching vibration [20, 21]. The band present at 1114 cm^{-1} is due to the (C-O) stretching vibrations which corresponds to the secondary alcohol. The band at 1069 cm^{-1} is due to C-C stretching vibration [22, 23]. The band at 897 cm^{-1} corresponds to C-H bending vibration which corresponds to alkene groups. The band at 599 and 509 cm^{-1} corresponds to deformation δ (COO^-) [24]. The Zn-O stretching vibration band was found at 435 cm^{-1} for ZnO-GW NPs [21, 22, 25]. The shifts in Zn-O band is due to the variations of biomolecules present in the bael fruit extract. FT-IR spectra of ZnO-GW confirmed that the prepared nanoparticles were coated with bio-molecules which were responsible for the reduction of zinc acetate and the prevention of the nanoparticles against oxidation. In *Adansonia digitata*, the hydroxyl groups of phenols and amide groups of proteins have been shown to act as capping agent which prevented agglomeration and provided stability to the nanoparticles [26]. Thus, from the IR spectrum it is evident that the biomolecules present in

the fruit extract of *Aegle marmelous* plays a major role in the reduction as well as stabilization of ZNO GW nanoparticles.

3.4 X-ray diffraction analysis (XRD) of ZnO-GW nanoparticles

XRD patterns showed the ZnO-GW NPs were semi-crystalline in nature. The XRD result for the ZnO GW nanoparticles shows the tendency of the three most intense diffraction peaks. The peaks for the synthesized ZnO-GW NPs were observed at scattering angle (2θ) of 23.96, 24.68, and 24.33. The crystalline ZnO nanoparticles displayed sharp and intense diffraction peaks that perfectly matched with the standard JCPDS file no:00-027-1401 -. It shows the presence of miller indices of (100), (002), (101), (102) and sharp peaks in the diffraction pattern indicates the purity of the product (Figure 4). The peaks of ZnO-GW NPs were broadened that may be due to the binding of ZnO with bio-molecules present in the bael fruit extract. The average crystallite size (D in nm) of ZnO-GW NPs was determined from XRD pattern from diffraction peak full width at half maximum (FWHM) according to the Debye – Scherrer equation (2)

$$D = K\lambda/\beta \cdot \cos\theta \tag{2}$$

Where K is Scherrer constant (0.9), it can be affected with the lattice direction and crystallite morphology. λ is the wavelength of the target Cu-Kα = 1.54 A. β refers to the peak width at half maximum (FWHM) which is determined in radians. θ is the diffraction angle based on the Scherrer equation, the average grain size at scattering angle (2θ) 24.78 and 31.20 of ZnO-GW NPs nm, respectively. The average grain size of the biosynthesized AgNPs was determined as 24 to 38 nm and is in accordance with the results obtained in TEM studies. The sharp peaks clearly confirmed the crystalline nature of the synthesized nanoparticles which is in good agreement with the earlier reports. ZnO NP synthesized using *Aegle marmelos* fruit extract showed the miller indices at (100), (002) and (101) showed sharp peaks in diffraction pattern [27].

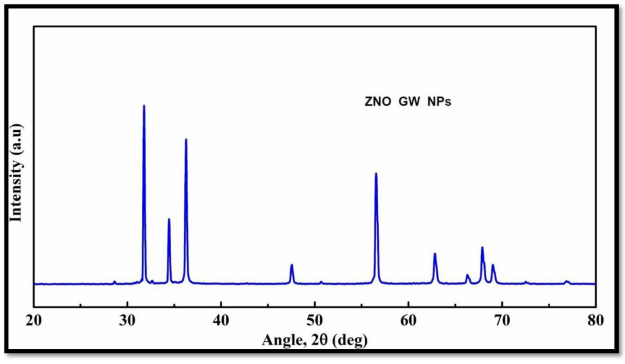

Figure 4: XRD peaks for ZnO GW nanoparticles prepared using *Aeglemarmelos* (Bael fruit).

3.5 High resolution transmission electron microscopic (HR-TEM)

Zn nanoparticles synthesized using *Euphorbia Jatropa* latex were hexagonal in shape and particles were in the size order of 500 nm [28]. The HR-TEM image showed the particles were polydispersed in nature (Figure 5). The TEM images of ZnO GW NPs prepared from the bael fruit extract were irregular cubic shapes with slight variations in thickness. The particle size was in the range of 50 nm and it agrees well with the average crystallite size calculated from the XRD pattern which in fact, makes the particles suitable for biological applications.

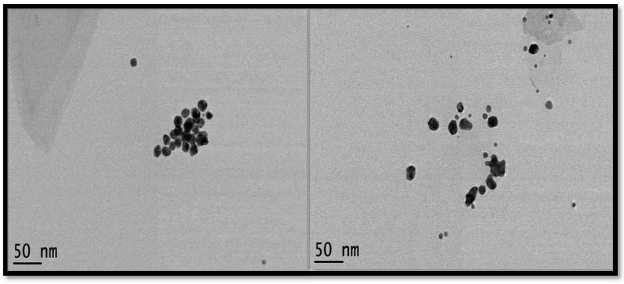

Figure 5: HR-TEM image of ZnO GW nanoparticles.

3.6 Cell proliferation assay

The cytotoxic studies of ZnO-GW NPs were investigated in MCF-7 cells by using MTT assay. Viability of MCF-7 cell lines was found to decrease with increase in concentration of ZnO-GW NPs as dose dependent manner (20 µg/ml – 100 µg/ml). The graph shows inhibition of cell proliferation in MCF-7 cell in dose depended manner (Figure 6). The MCF-7 cell proliferation was considerably lower, when compared to untreated (MCF-7) cell. After the treatment for 24 h and 48 h lower concentration (40 µg/ml and 60 µg/ml) killed more than 70% of cancer cells. The maximum inhibitions of cell proliferations were obtained at the concentration of (40 µg/ml) after 24 h and 48 h. The ZnO-GW NPs concentration at 40 µg/ml exhibited 87% cell viability and 60 µg/ml concentration showed 77% cell viability. It was observed from the results that ZnO-GW nanoparticles have imparted

a remarkable effect over MCF7 cells by creating cell damage, which agrees well with the literature [29]. NiO nanoparticles synthesized using *Aegle marmelos* leaf extract was shown to have cytotoxicity effect on A549 cell lines. The cell viability was observed to be 20% when treated with 1000 µg/mL of NiO nanoparticles and increased gradually to the maximum of 64.6% at the concentration of 7.8 µg/mL [30]. The exact mechanism for the cytotoxic effect of NP is not clearly known but few reports suggest that the metal ion which is released from the nano metal oxides plays a key role in cytotoxicity [31]. Hence the cytotoxicity of ZnO GW NP synthesized from *Aegle marmelos* could be from the release of Zn ions which will induce higher cytotoxicity effects than the micron sized particles. Release of metal ion creates oxidative stress by supporting the movements of exogenous materials inside the cells. Different mechanisms have been proposed based on the metal ion release. This includes the activation of calcium dependant and stress-inducible signalling cascades, which interferes with DNA repair pathways and causes epigenetic changes [32, 33]. The excess production of reactive oxygen species (ROS) and oxidative stress can cause DNA damage and apoptosis. The ROS production could damage the cell wall, DNA and eventually lead to cell death [34–36].

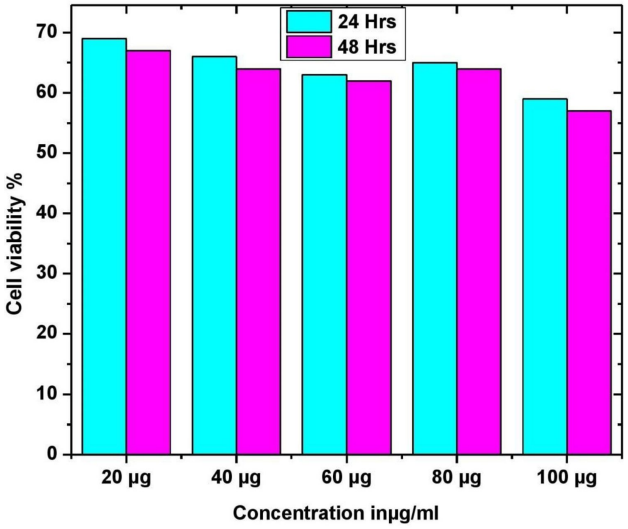

Figure 6: Cytotoxicity of different concentrations of ZnO GW NPs measured by MTT assay on MCF-7 cell lines.

4 Conclusion

Green synthesis of nanoparticles by biological systems especially plant extracts has become an emerging field in nanotechnology. In this study, zinc oxide nanoparticles were synthesized using *Aegle marmelos* L. fruit extract. UV-Vis spectrum showed the characteristic peak at 385 nm. FT-IR spectra of ZnO-GW NPs confirmed the group's characteristics of plant metabolite which were liable for the reduction of zinc acetate to ZnO-GW NPs. The manifestation of the optical absorption peak of UV-Vis spectral analysis proves the synthesis of ZnO GW nanoparticles. XRD pattern evidently illustrated the high crystallinity of the nanoparticles and the peaks of ZnO-GW NPs were broadened and weakened which may be due to the binding of ZnO with bio-component groups of bael fruit extract. The nanoparticle was found to be cytotoxic to MCF-7 tumor cells and has abridged the viability in MTT assay. ZnO GW NPs were found to be superior anticancer agents, a greenway technique for the synthesis of ZnO GW NPs is proposed for future studies. This pristine method is rapid, facile, convenient, less time-consuming, and environmentally safe. The process for the synthesis of nanoparticles on large scale using these readily available plant extracts may have commercial viability and would develop studies in the interface between biology and material science. Hence, the biological method of developing silver nanoparticles would be a cost-effective alternative to other approaches.

Acknowledgement: The author Dr. D.Manikandan acknowledges and gratefully to The Dr.Dun Yang, President & CEO at Anticancer Bioscience and Dr.Jing Zhang VP at Anticancer Bioscience ,Ltd., Chengdu 610000, China. The author Dr.S.U.Mohammed Riyaz acknowledge the Animal Tissue culture Unit, PG & Research Department of Biotechnology, Islamiah College (Autonomous), Vaniyambadi – 635752 for cell culture studies.

Funding information: The research was funded by UGC – Autonomous funding for PG & Research Department of Biotechnology, Islamiah College (Autonomous), Vaniyambadi – 635752.

Authors' contribution: D.M. – Conceptualization; D.M., M.S., B.K.K. - Data curation; D.M., M.S. - Formal Analysis; D.M., S.U.M.R. - Investigation; D.M. – Methodology; D.M. – Software; D.M., M.S. – Supervision; S.U.M.R. – Validation; D.M., M.S. - Writing -original draft; D.M., S.U.M.R., M.S. - Writing – review & editing

Conflict of interests: There is no conflict of interests

Ethical approval: The conducted research is not related to either human or animal use

Data availability statement: The datasets generated during and/or analysed during the current study are available from the corresponding author on reasonable request. Data sharing is not applicable to this article as no datasets were generated or analysed during the current study.

References

[1] Capek I, editor. Nanotechnology and nanomaterials. Stud. Interface Sci. Volume 23. Elsevier; 2006. pp. 1–69.

[2] Bayda S, Adeel M, Tuccinardi T, Cordani M, Rizzolio F. The History of Nanoscience and Nanotechnology: From Chemical-Physical Applications to Nanomedicine. Molecules. 2019 Dec;25(1):112.

[3] Mody VV, Siwale R, Singh A, Mody HR. Introduction to metallic nanoparticles. J Pharm Bioallied Sci. 2010 Oct;2(4):282–9.

[4] Khandel P, Yadaw RK, Soni DK, Kanwar L, Shahi SK. Biogenesis of metal nanoparticles and their pharmacological applications: present status and application prospects. J Nanostructure Chem. 2018;8(3):217–54.

[5] Espitia PJP, Soares N de FF, Coimbra JS dos R, de Andrade NJ, Cruz RS, Medeiros EAA. (2012) Zinc Oxide Nanoparticles: Synthesis, Antimicrobial Activity and Food Packaging Applications. Food Bioprocess Technol; 5:1447–64

[6] Jiang J, Pi J, Cai J. The Advancing of Zinc Oxide Nanoparticles for Biomedical Applications. Bioinorg Chem Appl. 2018 Jul;2018:1062562.

[7] Raveendran P, Fu J, Wallen SL. Completely "green" synthesis and stabilization of metal nanoparticles. J Am Chem Soc. 2003 Nov;125(46):13940–1.

[8] Baliga MS, Bhat HP, Joseph N, Fazal F. Phytochemistry and medicinal uses of the bael fruit (Aegle marmelos Correa): A concise review. Food Res Int. 2011;44(7):1768–75.

[9] Rahman S, Parvin R. Therapeutic potential of Aegle marmelos (L.)-An overview. Asian Pac J Trop Dis. 2014;4(1):71–7.

[10] Baliga MS, Mane PP, Joseph N, Jimmy R. Chapter 20: Review on the Protective Effects of the Indigenous Indian Medicinal Plant, Bael (*Aegle marmelos* Correa), in Gastrointestinal Disorders. In: Watson RR, Preedy VR, editors. Bioact. Food Diet. Interv. Liver Gastrointest. Dis. San Diego: Academic Press; 2013. pp. 313–24.

[11] N D Krupa A. Raghavan V. Biosynthesis of Silver Nanoparticles Using. *Aegle marmelos* (Bael) Fruit Extract and Its Application to Prevent Adhesion of Bacteria: A Strategy to Control Microfouling. 2014. Bioinorg Chem Appl. 2014;e949538.

[12] Rao KJ, Paria S. *Aeglemarmelos* Leaf Extract and Plant Surfactants Mediated Green Synthesis of Au and Ag Nanoparticles by Optimizing Process Parameters Using Taguchi Method. ACS Sustain Chem& Eng. 2015;3(3):483–91.

[13] Devi M, Devi S, Sharma V, Rana N, Bhatia RK, Bhatt AK. Green synthesis of silver nanoparticles using methanolic fruit extract of *Aegle marmelos* and their antimicrobial potential against human bacterial pathogens. J Tradit Complement Med. 2019 May;10(2):158–65.

[14] Mallikarjunaswamy C, Lakshmi Ranganatha V, Ramu R, Udayabhanu, Nagaraju G. Facile microwave-assisted green synthesis of ZnO nanoparticles: application to photodegradation, antibacterial and antioxidant. J Mater Sci Mater Electron. 2020;31(2):1004–21.

[15] Geetha MS, Nagabhushana H, Shivananjaiah HN. Green mediated synthesis and characterization of ZnO nanoparticles using Euphorbia Jatropa latex as reducing agent. Journal of Science: Advanced Materials and Devices. 2016;1:301–10.

[16] Ramadoss G, Suriyaraj SP, Sivaramakrishnan R, Pugazhendhi A, Rajendran S. Mesoporous ferromagnetic manganese ferrite nanoparticles for enhanced visible light mineralization of azoic dye into nontoxic by-products. Sci Total Environ. 2021 Apr;765:142707.

[17] Bahadar H, Maqbool F, Niaz K, Abdollahi M. Toxicity of nanoparticles and an overview of current experimental models. Iran Biomed J. 2016;20(1):1–11.

[18] Shen C, James SA, de Jonge MD, Turney TW, Wright PF, Feltis BN. Relating cytotoxicity, zinc ions, and reactive oxygen in ZnO nanoparticle-exposed human immune cells. Toxicol Sci. 2013 Nov;136(1):120–30.

[19] Zhang Y, Bai Y, Jia J, Gao N, Li Y, Zhang R, et al. Perturbation of physiological systems by nanoparticles. Chem Soc Rev. 2014 May;43(10):3762–809.

[20] Sohaebuddin SK, Thevenot PT, Baker D, Eaton JW, Tang L. Nanomaterial cytotoxicity is composition, size, and cell type dependent. Part Fibre Toxicol. 2010 Aug;7(1):22.

[21] Pujalté I, Passagne I, Brouillaud B, Tréguer M, Durand E, Ohayon-Courtès C, et al. Cytotoxicity and oxidative stress induced by different metallic nanoparticles on human kidney cells. Part Fibre Toxicol. 2011 Mar;8(1):10.

[22] Khanna P, Ong C, Bay BH, Baeg GH. Nanotoxicity: an interplay of oxidative stress, inflammation and cell death. Nanomaterials (Basel). 2015 Jun;5(3):1163–80.

[23] Fu PP, Xia Q, Hwang HM, Ray PC, Yu H. Mechanisms of nanotoxicity: generation of reactive oxygen species. J Food Drug Anal. 2014 Mar;22(1):64–75.

[24] Kroemer G, Galluzzi L, Brenner C. Mitochondrial membrane permeabilization in cell death. Physiol Rev. 2007 Jan;87(1):99–163.

[25] Kumar CM, Yugandhar P, Savithramma N. Biological synthesis of silver nanoparticles from *Adansonia digitata* L. fruit pulp extract, characterization, and its antimicrobial properties J.IntercultEthnopharma col. 2016; 5(1): 79-8526.

[26] Anupama C, Kaphle A, Udayabhanu, Nagaraju G. Aegle marmelos assisted facile combustion synthesis of multifunctional ZnO nanoparticles: study of their photoluminescence, photo catalytic and antimicrobial activities. J Mater Sci Mater Electron. 2018 Mar;29(5):4238–4249.

[27] Geetha MS, Nagabhushana H, Shivananjaiah HN. Green mediated synthesis and characterization of ZnO nanoparticles using *Euphorbia Jatropa* latex as reducing agent. Journal of Science: Advanced Materials and Devices. 2016;1(3):301–10.

[28] Mariam AA, Kashif M, Arokiyaraj S. Bio-synthesis of NiO and Ni nanoparticles and their characterization. Dig J Nanomater Biostruct. 2014;9:1007–19.

[29] Angel Ezhilarasi J, Judith Vijaya K. Kaviyarasu, L. John Kennedy, R. Jothiramalingam, Hamad A. Al-Lohedan Green synthesis of NiO nanoparticles using *Aeglemarmelos* leaf extract for the evaluation of in-vitro cytotoxicity, antibacterial and photocatalytic

properties. J Photochem Photobiol B. 2018;180:39–50.
[30] Horie M, Nishio K, Fujita K, Endoh S, Miyauchi A, Saito Y, et al. Protein adsorption of ultrafine metal oxide and its influence on cytotoxicity toward cultured cells. Chem Res Toxicol. 2009 Mar;22(3):543–53.
[31] Begum S, Sultana R, Siddiqui BS. Triterpenoids from the leaves of*Neriumoleander*. Phytochemistry. 1997;44(2):329–32.
[32] Siddiqui BS, Khatoon N, Begum S, Farooq AD, Qamar K, Bhatti HA, et al. Flavonoid and cardenolide glycosides and a pentacyclic triterpene from the leaves of*Nerium oleander* and evaluation of cytotoxicity. Phytochemistry. 2012 May;77:238–44.
[33] Tahir K, Nazir S, Li B. UllahKhan A, HaqKhan Z.U, Yu P, Gong S, UllahKhan S, Ahmad A U. Biodirected synthesis of palladium nanoparticles using *Phoenix dactylifera* leaves extract and their size dependent biomedical and catalytic applications. Mater Lett. 2016;6(89).
[34] Jayaprakash N, Judith Vijaya J, Kaviayarasu K, Kombaiah K, John Kennedy L, Jothiramalingam R, et al. Munusamy, Hamad A Al-Lohedan. Green synthesis of Ag nanoparticles using Tamarind fruit extract for the antibacterial studies. J PhotochemPhotobio B Bio. 2017;169: 178-18535.
[35] Kaviyarasu K, Kennedy J, Manikandan E, Henini M, Maaza M. Photodegradation of organic pollutants RhB dye using UV simulated sunlight on ceria based TiO2 nanomaterials for antibacterial applications. Sci Rep. 2016;6:38064.
[36] Kaviyarasu K, Kanimozhi K, Matinise N. Maria magdalane C, Mola GT, Kennedy J, Maaza M. Antiproliferative effects on human lung cell lines A549 activity of cadmium selenide nanoparticles extracted from cytotoxic effects: investigation of bioelectronic application. Mater Sci Eng C. 2017;76:1012–25.